Identification and Characterization of Kink Motifs in 1-Palmitoyl-2-Oleoyl-Phosphatidylcholines: A Molecular Mechanics Study

Shusen Li, Hai-nan Lin, Zhao-qing Wang, and C. Huang
Department of Biochemistry, Health Sciences Center, University of Virginia, Charlottesville, Virginia 22908 USA

ABSTRACT As a *cis* carbon-carbon double bond (Δ) is introduced into the middle of an isolated all-*trans* hydrocarbon chain, it can be shown by molecular graphics that this Δ-bond makes a bend of 130° in the chain axis, thus producing a boomerang-like conformation. Such a bent structure, indeed, has been detected experimentally for oleic acid by x-ray crystallography (Abrahamson and Ryderstedt-Nahringbaur, 1962). Membrane diacyl phospholipids are largely mixed-chain lipids containing a saturated *sn*-1 acyl chain and an unsaturated *sn*-2 acyl chain. 1-Palmitoyl-2-oleoyl-phosphatidylcholine (POPC), the most abundant phospholipid in animal cell membranes, is a typical example in which the *sn*-2 acyl chain is the acyl chain of an oleic acid. However, this *sn*-2 acyl chain of POPC is unlikely to adopt a boomerang-like configuration in the gel-state lipid bilayer due to the steric hindrance imposed by neighboring chains. Instead, it has been suggested that the oleate chain in POPC is kinked in the shape of a crankshaft in the gel-state bilayer (Huang, 1977; Lagaly et al., 1977), because POPC with such a kinked *sn*-2 acyl chain, which is denoted here as the secondary structural element or motif, can pack efficiently against other neighboring phospholipids. In this communication, 16 different types of secondary structural elements or motifs are derived for POPC at $T < T_m$ based on a single protocol guided by two-dimensional steric contour maps and computer-based molecular graphics. After subjecting these derived molecular species to energy minimization using the molecular mechanics method, the number of the secondary structural motifs is reduced to 13 as a result of conformational degeneracy. The structure and steric energy of each of the energy-minimized lipid rotomers are presented in this communication. Furthermore, these rotomers packed in small clusters are also simulated to mimic the lipid bilayer structure of 1-palmitoyl-2-oleoyl-phosphatidylcholines at $T < T_m$.

INTRODUCTION

Phospholipids, quantitatively the most important lipids isolated from biological membranes, consist of two parts: the headgroup and the diglyceride moiety. The diglyceride moiety usually contains two long hydrocarbon chains attached via ester/ester, ester/ether, or ether/ether linkages to the carbon atoms 1 and 2 of the glycerol backbone, respectively. The one linked to the glycerol carbon atom 1, the *sn*-1 chain, is often a saturated hydrocarbon chain with repeated methylene units between 14 and 24, whereas the other, the *sn*-2 chain, is frequently an unsaturated hydrocarbon chain containing *cis* carbon-carbon double bonds ranging from 1 to 6.

Synthetic phospholipids with two long polymethylene chains such as dimyristoyl- and dipalmitoyl phosphatidylcholines have been studied extensively over the years as model membrane lipids (Huang, 1991). When these synthetic phospholipids are dispersed in aqueous media at a concentration greater than the critical micellar concentration, they tend to self-assemble into an organized supermolecular structure known as the liposome. After prolonged incubation of the liposome at 0°C, all lipid molecules packed in the liposome reach the equilibrium state. In this state, the long polymethylene chains of each lipid molecule adopt the minimum potential energy conformation that corresponds to a fully extended all-*trans* configuration. Upon heating to a characteristic temperature, the polymethylene chains of each self-assembled lipid molecule are "energized"; the packing of the hydrocarbon chain will involve some general loosening but will maintain the overall straight configuration. This thermally induced loosening of the molecular packing is accompanied by a molar volume increase, arising mainly from the *trans*→*gauche* isomerizations of carbon-carbon single bonds along the polymethylene chains within each lipid molecule. However, to maintain even approximately the overall straight chain configuration, the conformational disordering process of *trans*→*gauche* isomerizations must be constrained and limited to certain coupled rotations. Of the various coupled isomerizations, the sequential g^+tg^- and g^-tg^+ bonds, known as the 2g1 kink, are best characterized (Pechhold and Blassenbrey, 1967; 1970). Here g^+, t, and g^- are the *gauche*$^+$, *trans*, and *gauche*$^-$ conformation, respectively, of a carbon-carbon single bond in a hydrocarbon chain. Using the ball-and-stick molecular model, these three conformations can be conveniently recognized by looking down on the chain axis of a segment of four methylene units [-C(1)H_2-C(2)H_2-C(3)H_2-C(4)H_2-], in which C(1) and C(4) atoms are aligned in an eclipsed position and at 12 on the clock face. A rotation of 60° of C(3) atom around the C(2)-C(3) bond in the clockwise direction, or a torsion angle of +60°, results

Received for publication 8 November 1993 and in final form 9 February 1994.

Address reprint requests to Ching-hsien Huang, Department of Biochemistry, Box 440, Health Sciences Center, University of Virginia, Charlottesville, VA 22908. Tel.: 804-924-5010; Fax: 804-924-5069.

Abbreviations used: C(14):C(14)PC, L-α-dimyristoyl-phophatidylcholine; Δ, the *cis* carbon-carbon double bond; E_s, the steric energy, obtained with the computer software MM2 (Version 85), corresponding to the energy-minimized structure of the calculated molecule; MM, molecular mechanics; POPC, 1-palmitoyl-2-oleoyl-phosphatidylcholine; T_m, the main phase transition temperature.

0006-3495/94/06/2005/14 $2.00

in the formation of a g^+ conformation. A counterclockwise rotation of 60°, or a torsion angle of −60°, gives rise to a g^- conformation. Rotation of a torsion angle of either +180 or −180° produces the t conformation. If a g^+ bond and a g^- bond are simultaneously formed along an all-*trans* hydrocarbon chain and they are separated by a t bond, this coupled g^+tg^- sequence will convert the fully extended hydrocarbon chain into a two-segment chain. These two segments are co-linear with each other. Geometrically, the hydrocarbon chain is kinked in the shape of a crankshaft. Overall, the chain length is shortened by 1.27 Å but laterally expanded by 1.86 Å. The sequence g^+tg^- can be regarded as the sequence for a secondary structural element or motif for hydrocarbon chain. The occurrence of such a kinked motif in a closely packed hydrocarbon chain is quite common (Lagaly, 1976; Yeagle, 1993). Interestingly, the sequence g^+tg^- of a saturated lipid acyl chain has been implied to constitute a mobile site in the bilayer interior to carry a water molecule across the lipid bilayer (Traüble, 1971). In this paper, we denote the hydrocarbon chain having a crankshaft-like topology as the secondary structural element or motif and the local kinked region as the crankshaft-like kink or simply kink.

In contrast to synthetic phospholipids described above, naturally occurring phospholipids usually are mixed-chain phospholipids containing one or more *cis* carbon-carbon double bonds. 1-Palmitoyl-2-oleoyl-phosphatidylcholine (POPC) is a typical example. The introduction of a *cis* carbon-carbon double bond (Δ) into a hydrocarbon chain enables the chain to adopt a large number of interconverting conformations. This added conformational variability can facilitate, in turn, the formation of the secondary structural elements, provided that the Δ-containing chain is packed in an organized structure such as the gel-state lipid bilayer. Specifically, the sequence Δtg^- (or $g^+t\Delta$) has been proposed to form a crankshaft-like kink around the *cis* carbon-carbon double bond in the *sn*-2 acyl chain of POPC (Huang, 1977). This type of Δ-containing kink can generate adjustable hydrophobic pockets in the bilayer interior; moreover, the pocket architecture has the proper geometric features to accommodate nicely the two angular methyl groups of cholesterol molecule protruding from the β-surface of the steroid nucleus (Huang, 1977). The presence of Δ-containing kinks in a lipid acyl chain, therefore, may have profound effects on the lipid-lipid interactions in biological membranes.

Although Δ-containing kinks have been proposed to occur in mixed-chain phospholipids such as 1-palmitoyl-2-oleoyl phosphatidylcholine since 1977 (Huang, 1977), our current knowledge about the various types of Δ-containing kinks and their detail conformations in membrane mixed-chain lipids is still scanty. This is largely because mixed-chain phospholipids with an unsaturated acyl chain are notoriously difficult to crystallize and, hence, no x-ray crystallographic data are available. However, the advance made recently in the computer-based molecular mechanics together with the availability of fast computers has made it possible to carry out the lengthy molecular mechanics (MM) calculations and, hence, the successful determinations of the conformations and energies of phospholipids packed in various states (Vanderkooi, 1991; Nakata et al., 1992; Li et al., 1993). In the absence of any crystal structural determination of phospholipids with unsaturated acyl chains, we are compelled to take the computer-based molecular mechanics calculations as the next best approach in searching for the Δ-containing kinks and in determining the conformation and energy of the various secondary structural motifs in the gel-state phospholipid bilayer.

In this communication, four basic groups of the secondary structural elements obtained with POPC at $T < T_m$ are given. Within each group, there are three or four types of Δ-containing kinks. Most interestingly, one of the Δ-containing kinks found by our MM calculations is virtually indistinguishable from the energy-minimized kink derived from the one found crystallographically in the oleate chain of cholesteryl oleate at 123 K as determined by x-ray diffraction (Gao and Craven, 1986). This complete agreement lends strong support to the validity of our MM approach.

COMPUTATIONS

The software MM2 (Version 85), a molecular mechanics program originally developed by Allinger (1977), was used to compute the atomic coordinates and the steric energy of the energy-minimized structure of the diglyceride moiety of the mixed-chain phospholipid, as described in our earlier work (Li et al., 1993). In this program, the steric energy consists of the bond stretching, bond-angle bending, torsional, bond dipole or atomic charge, van der Waals, and bond stretch and angle bending cross terms. Of the various terms, the van der Waals term, E_{VDW}, plays the most important role in determining the diglyceride moiety structure and the steric energy of the lipid molecule. In the MM2 program, van der Waals interactions include atoms with 1–4 vicinal and more relationships as described previously (Li et al., 1993).

In addition, the simulations of tetramers of lipid molecules in a box surrounded by 26 replicas of image boxes by using periodic boundary conditions were carried out with the software package HyperChem (Autodesk, Sausalito, CA). The MM$^+$ program of HyperChem was used occasionally in this work as stated in the text. Furthermore, HyperChem was used to display visually the three-dimensional structures of lipids by showing calligraphic or raster graphics and to align the lipid molecules into dimers or tetramers prior to energy minimizations.

RESULTS AND DISCUSSION

The *cis* carbon-carbon double bond and its effects on the hydrocarbon chain

A fragment of a long all-*trans* hydrocarbon chain containing a *cis* carbon-carbon double bond is shown in Fig. 1 *A*, illustrating the notations used here in numbering the carbon atoms and the associated torsion angles. The two olefinic carbon atoms linked by the *cis* carbon-carbon double bond are designated as C_i and C_j, and the *cis* double bond itself is denoted by Δ with a torsion angle of 0°. The torsion angles of carbon-carbon single bonds preceding the C_i are designated as δ_n, where the subscript n is the number of the carbon-carbon single bond counting away from C_i as shown in Fig. 1 *A*. Similarly, the torsion angles of carbon-carbon single bonds succeeding C_j are designated as δ'_n.

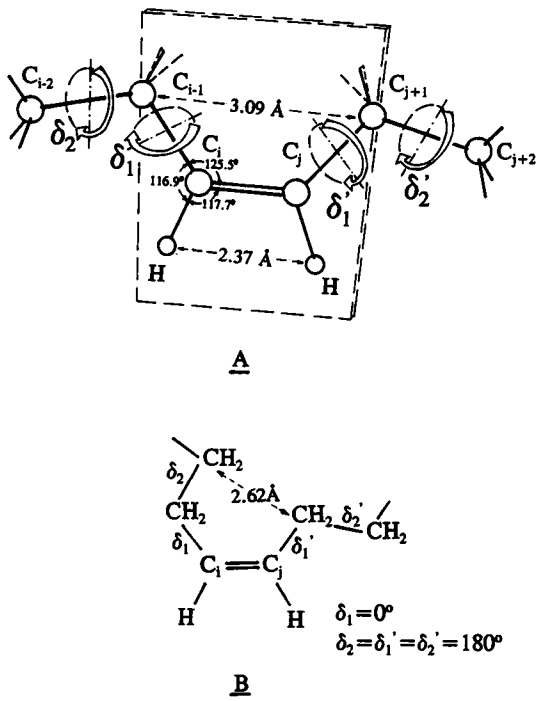

FIGURE 1 Structure of a *cis* carbon-carbon double bond within a segment of a hydrocarbon chain. (*A*) The six-atom structural unit is diagrammatically illustrated; the bond angles and bond distances within the planar six-atom structural unit are also given. The torsion angles of all the carbon-carbon single bonds are 180° ($\delta_1 = \delta_2 = \delta_1' = \delta_2' = 180°$). (*B*) The same structure as *A*, except that the δ_1-torsion angle is 0°.

Using the designations of δ_1 and δ_n'-angles just given, the conformation of the chain segment shown in Fig. 1 *A* can then be specified by $\delta_1 = \delta_1' = 180°$. This conformation shown in Fig. 1 *A* is in fact under steric strain, because the C_{i-1}-methylene and C_{j+1}-methylene carbons are in too close proximity (3.09 Å). Another example is illustrated in Fig. 1 *B*, in which the δ_1 and δ_1' angles are 0° and 180°, respectively. In this case, the spatial distance between the C_{i-2}-methylene and C_{j+1}-methylene carbons would be 2.62 Å, which is considerably less than the sum of the van der Waals radii of the carbon atoms involved (3.80 Å); consequently, this conformation is disallowed sterically.

The *cis* carbon-carbon double bond is a rigid linkage owing to the presence of both σ and π bonds between the two olefinic carbon atoms. As a result, rotation of C_i and C_j atoms around the rigid linkage is prohibited energetically at the physiological temperature, and the six atoms, C_{i-1}, C_i-H, C_j-H, and C_{i+1}, surrounding the rigid linkage are fixed in a common plane with relatively constant bond lengths and bond angles as depicted in Fig. 1 *A*. Because of the planar configuration, these six atoms constitute a basic structural unit that is referred to here as the six-atom structural unit. When a *cis* carbon-carbon double bond is introduced into a long all-*trans* hydrocarbon chain, it exerts significant effects on the conformation and dynamics of the long hydrocarbon chain. Before we present the data, it is pertinent to discuss first briefly the conformation and steric energy of an isolated saturated hydrocarbon chain.

Fig. 2 *A* shows the lowest-energy conformation of a saturated hydrocarbon chain, *n*-dodecane, in which each methylene unit repeats at regular intervals and is arranged in congruence with its neighboring methylene units along the chain by a rotation of 180° about the carbon-carbon single bond and a translation of 1.27 Å along the common molecular axis. This all-*trans* conformation is the most stable structure because the steric repulsion between the methylene units along the chain axis is minimal. The potential (or steric) energy of this all-*trans* conformation, obtained by MM calculations, is 7.29 kcal/mol. As carbon atom 7 or C(7) rotates progressively from 180° to −180° around the single bond between C(6) and C(7) atoms, the potential energy obtained from the MM2 program shows a systematic change, resulting in three potential energy maxima separated by three potential energy minima (Fig. 3). The two minima at torsion angles of +65° and −65° correspond to the conformations in which two carbon atoms linked to C(6) and C(7) atoms are *gauche*$^+$ and *gauche*$^-$, respectively. The conformation of dodecane with a g^+ bond at C(6)-C(7) position is illustrated in Fig. 2 *B*. The potential energy profile, depicted in Fig. 3, also shows that an energy barrier of 3.33 kcal/mol has to be overcome in rotating the C(6)-C(7) bond in dodecane from the *t* to the g^+ conformation; furthermore, the potential energy difference between the *t* and the g^+ conformation is 0.92 kcal/mol.

When a *cis* carbon-carbon double bond is introduced into *n*-dodecane between C(6) and C(7) atoms, the linear hydrocarbon chain is changed to a bent configuration with an obtuse angle of about 130° in the chain axis as indicated by the computer graphics of *cis* dodecene-6 presented in Fig. 2 *C*. Most interestingly, the bend at the double bond, when viewed from the edge, bears a strong resemblance to the bend generated by a *gauche*$^+$ (or *gauche*$^-$) bond in dodecane at the corresponding position (Fig. 2 *B*). When viewed down the hydrocarbon chain axis, however, the two segments separated by the g^+ (or g^-) bond in the dodecane rotamer can be seen to orient at different directions, whereas the two segments separated by the *cis* double bond in *cis* dodecene-6 line up along the chain axis to form a curved tandem.

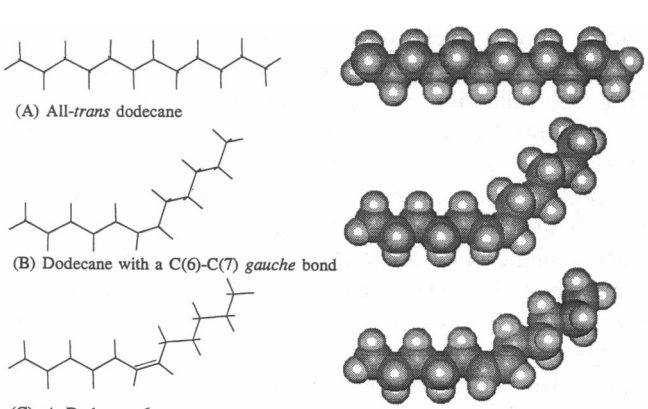

FIGURE 2 Computer-graphics representations of the structures of all-*trans* dodecane (*A*), dodecane with a C(6)-C(7) gauche bond (*B*), and *cis* dodecene-6 (*C*). The wire and sphere models are presented for each structure.

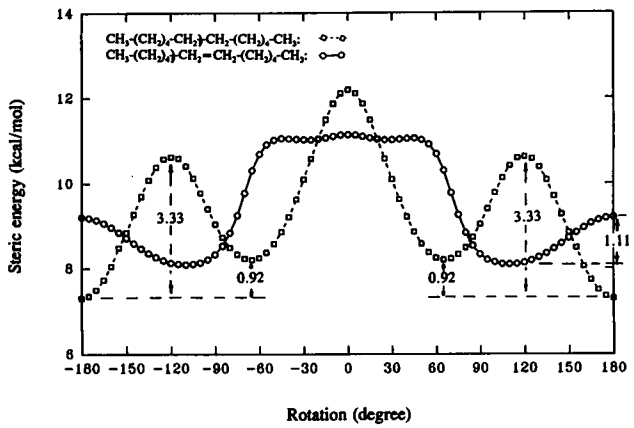

FIGURE 3 The steric energy changes arising from rotation of the C(6)-C(7) bond of dodecane (□), and from rotation of the C(4)-C(5) bond of *cis* dodecene-6 (○). Calculations were executed with the force field Allinger method using the MM2 program (Version 85). The unit for the energy difference is kcal/mol as indicated.

In addition to bending the chain, the presence of a *cis* carbon-carbon double bond in a hydrocarbon chain can confer rotational flexibility upon the two carbon-carbon single bonds in the six-atom structural unit. The torsion angles of these two bonds are designated as δ_1 and δ_1' (Fig. 1). MM calculations were performed to determine the potential energy of *cis* dodecene-6 as a function of δ_1-angle. In these MM calculations, all other degrees of freedom were initially taken as 180° (i.e., $\delta_n = \delta_n' = 180°$) followed by flexible geometry except that $\delta_1' = 180°$ as the study about the rotational bond (δ_1-angle) was to traverse, using 5° increments, a full (−180 to 180°) cycle. Results obtained with the rotator about δ_1-angle are also presented in Fig. 3. It is evident from Fig. 3 that the energy profile is characterized by a very broad peak ranging from −60° to +60° and a much narrower but considerably smaller peak centered at 180° (Fig. 3). The maximal peak at $\delta_1 = 0°$ corresponds to the energetically disallowed conformation of *cis* dodecene-6 shown in Fig. 1 *B*. In addition, two broad subsidiary minima centered at $\delta_1 = \pm 110°$ are discernible. An energy barrier of 1.11 kcal/mol to rotation of the carbon-carbon single bond between the two energy minima is detected (Fig. 3). This value is 2.22 kcal/mol less than the calculated energy barrier to rotation of the same carbon-carbon single bond in an equivalent hydrocarbon chain without the presence of a double bond. Our MM calculations thus provide quantitative information indicating that the carbon-carbon single bond adjacent to a rigid *cis* carbon-carbon double bond is considerably more flexible in rotation than the normal carbon-carbon single bond due to the smaller energy barrier. It is worthwhile to point out that Fig. 3 shows two very broad potential energy wells over the δ_1 range of +85° to +140° and −85° to −140° for *cis* dodecene-6. This is of particular interest because the largest difference in potential energy within the well is of the order of 0.4 kcal/mol. The magnitude of this energy difference approximates the average kinetic energy of the thermal environment at −72°C (~*RT*), suggesting that the carbon-carbon single bond adjacent to the double bond can undergo angular oscillation over a wide range of rotational angles as a consequence of thermal fluctuations. Based on MM calculations, one can conclude that the two segments of the hydrocarbon chain separated by the planar six-atom structural unit can adopt a wide variety of stable configurations at temperatures far below 0°C.

Potential-energy calculations and the two-dimensional steric contour maps

As pointed out in the Introduction, the successive g^+tg^- and g^-tg^+ bonds in a polymethylene chain are, respectively, well established kink-forming sequences. These sequences are regarded here as the reference or template sequences in the search for other kinks. For instance, computer graphics show that the conformation of a *gauche*-rotamer derived from a saturated hydrocarbon chain (Fig. 2 *B*) is remarkably similar, in the X-Y plane, to that of a Δ-containing hydrocarbon chain (Fig. 2 *C*). Consequently, if one of the two *gauche* bonds in the reference sequence g^+tg^-, say, one on the left, is substituted by a Δ-bond, then the resulting new sequence, Δtg^-, may have the kink-forming propensity. However, the conformation of a *gauche*$^-$ rotamer is not completely identical to that of the Δ-containing hydrocarbon chain, especially when viewed down the chain axis. Hence, the various torsion angles associated with the sequence Δtg^- need to be modified somewhat to make it a truly kink-forming sequence. Given the facts that the torsion angle of Δ is essentially fixed at 0°, and that the carbon-carbon single bonds adjacent to a *cis* carbon-carbon double bond are highly flexible, the adjustments needed for the sequence Δtg^- can be assigned to the set of (δ_1', δ_2')-angles with a more flexible δ_1'-angle. The next step is then to guess a crude set of (δ_1', δ_2')-angles in the Δtg^- sequence which, to a first approximation, is able to convert the unsaturated hydrocarbon chain into a crankshaft-like chain. A more accurate set of (δ_1', δ_2')-values can then be obtained from MM calculations based on the guessed values of (δ_1', δ_2')-angles.

In an attempt to find an appropriate set of (δ_1', δ_2')-torsion angles in the sequence Δtg^- that can generate a crankshaft-like kink and, at the same time, that this set of torsion angles is in the sterically allowed region in the (δ_1', δ_2')-plane, MM calculations have been undertaken to generate the two-dimensional steric contour (δ_1', δ_2')-map for the molecular structure of *cis* dodecene-6. In this approach, the angles of δ_1' $(=\delta_1)$ and δ_2' $(=\delta_2)$ are each rotated in 15° increments over a full cycle of 0° to 360°. Specifically, the potential (or steric) energy of *cis* dodecene-6 with a fixed δ_2'-angle of 0° is computed as a function of δ_1'-angle, using 15° increments, in the range of −180° to 180°. After every 15°-bond rotation of δ_1'-angle, the molecular structure of *cis* dodecene-6 is self-adjusted by a complete energy-minimization at the particular δ_1'-angle. The steric energy of each energy-minimized structure is then recorded. Move δ_2' to 15° and repeat the MM calculations again by rotating

the δ_1'-angle, via the 15° increment, through 360°. Record the energy-minimized steric energy again after each rotational increment. When δ_2' has been advanced through 360°, a total of 625 MM calculations with recorded steric energies have been performed.

The results of steric energy calculations are presented in the two-dimensional (δ_1', δ_2')-map given in Fig. 4 *A*. The steric energy contour zones are drawn at intervals of 0.5 kcal mol^{-1} near the minima. The maxima can be seen to occur at about (δ_1' = −15° to 15°, δ_2' = −30° to +30°), (δ_1' = −15° to 15°, δ_2' = 115° to 145°), and (δ_1' = −15° to 15°, δ_2' = 115° to 130°), corresponding to three regions of sterically disallowed domains. There are six distinct regions on the (δ_1', δ_2')-map marked with + in which the potential energies of *cis* dodecene-6 are minima; every two minima at the same level of δ_2'-value are surrounded by long shallow wells, indicating that there are large numbers of sterically allowable regions. This is a manifestation of the much greater conformational flexibility of the single carbon-carbon bonds adjacent to the Δ-bond in the six-atom structural unit.

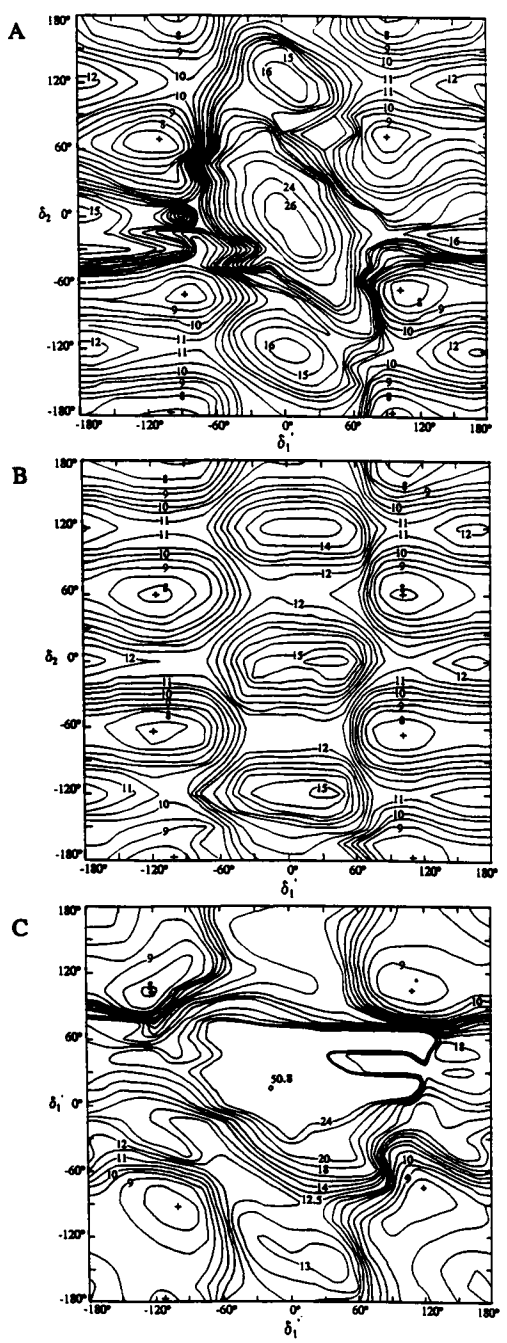

FIGURE 4 Steric contour maps for *cis* dodecene-6 resulting from rotations of (δ_1,δ_2)-torsion angles (*A*), (δ_1',δ_2)-torsion angles (*B*), and (δ_1, δ_1')-torsion angles with a fixed δ_2' value of 73° (*C*). The energy contour zones surrounding the minima (marked by +) are drawn at intervals of 0.5 kcal/mol. The numbers on the contour lines correspond to the values of steric energy in kcal/mol.

Because we are interested in finding out the combinations of (δ_1', δ_2')-angles in the sequence Δtg^- that may generate the crankshaft-like kink, *cis* dodecene-6 molecules with (δ_1', δ_2') values near the two potential energy minima with the δ_2'-angle of about −65° are examined by computer graphics. Results indicate that *cis* dodecene-6 structures with sets of (δ_1' = −90°, δ_2' = −75°), (δ_1' = 120°, δ_2' = −70°) give rise to bent conformations in which the two segments are bisected by about 120° and 90°, respectively. In fact, any positive δ_1' angle in the energetically allowed range of 30° to 180° will result in a bent conformation when it is introduced into the sequence Δtg^- with a fixed torsional angle of δ_2' = −65°. Hence, these positive values of torsion angles are ruled out as the appropriate torsional angles for the kink-forming sequence Δtg^-. If, on the other hand, a negative value of δ_1' is taken from the broad −90° to −165° range and is paired with δ_2' = −65° in the sequence Δtg^-, a crankshaft-like kink is generally observed based on computer graphics.

Search for Δ-containing kink models in an unsaturated sn-2 acyl chain in POPCs

The success of the combined application of steric-energy contour (δ_1', δ_2')-map and computer graphics in identifying the Δtg^- kink in *cis* dodecene-6 allows us to look for kink models in the *sn*-2 acyl chain of POPCs at temperatures below the phase transition temperature (T_m) of the lipid assembly. In this diacyl lipid molecule, the *sn*-1 acyl chain is considered to be an all-*trans* linear chain at $T < T_m$; it may impose steric hindrance and, hence, the energetic constraint to the neighboring *sn*-2 acyl chain. Consequently, the allowable sets of (δ_1', δ_2')-angles in the *sn*-2 acyl chain to form the crankshaft-like kink may be severely restricted in comparison with those observed in an isolated *cis* dodecene-6 molecule.

The atomic coordinates of the equilibrium diglyceride structure of C(14):C(14)PC in the gel-state bilayer reported by Li et al. (1993) are taken as the starting reference points to the deduction of the diglyceride moiety of POPC topologies packed in the gel-state bilayer at $T < T_m$. The fundamental structure of the diglyceride moiety of POPC deduced from the equilibrium structure of C(14):C(14)PC in the gel-state bilayer is presented in Fig. 5, *a* and *a'*. In this case, the

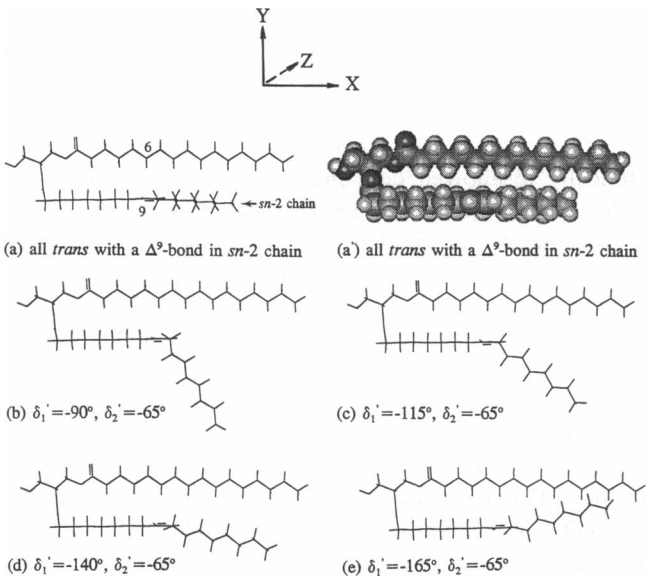

FIGURE 5 The computational screening of POPC structures with various kink-forming sequences. These sequences were originally obtained from isolated cis dodecene-6. (*a*) The deduced structure of the diglyceride moiety of mixed-chain POPC with an all *trans* *sn*-2 acyl chain containing a *cis* carbon-carbon double bond between C(9) and C(10) atoms. (*a'*) The same deduced POPC structure as illustrated in *a*, except that the atoms are shown as solid spheres of radius equal to the van der Waals radius. (*b–d*) The diglyceride moieties of POPC in which the *sn*-2 acyl chains have different sets of (δ_1', δ_2')-torsion angles as indicated.

sn-2 acyl chain of C(14):C(14)PC starting at C(3) atom is replaced by an all-*trans* sixteen-carbon hydrocarbon chain segment with a *cis* carbon-carbon double bond (torsion angle = 0°) between C(9) and C(10) atoms. In addition, the *sn*-1 acyl chain of C(14):C(14)PC is elongated by two methylene units, each connected by two carbon-carbon single bonds with torsion angles of 180°. Once the fundamental structure of the diglyceride moiety of POPC is deduced, it can then be used to incorporate individually the various kink-forming sequences with different guessed sets of torsion angles around the Δ-bond. It should be pointed out that the *sn*-2 acyl chain of POPC shown in Fig. 5, *a* and *a'* has a bent configuration. The lower segment bends downward from C(11) atom, projecting away from the viewer toward the back of the paper plane.

In the previous section, we have mentioned that if a negative value of δ_1' is taken from the broad −90° to −165° region of the two-dimensional (δ_1', δ_2')-map shown in Fig. 4 *A* and is then paired with $\delta_1' = -65°$ in the sequence Δtg^-, a crankshaft-like kink is generally observed in the molecular structure of *cis* dodecene-6. Based on these observations, computer graphics analyses of four structures of POPCs, constructed on the basis of four δ_1'-values (−90°, −115°, −140°, and −165°) and a fixed δ_2'-value of −65°, are undertaken. Examinations of the results shown in Fig. 5 *b–e* reveal clearly that the *sn*-2 acyl chain with a set of ($\delta_1' = -140°$, $\delta_2' = -65°$)-torsion angles is the only one that can form a crankshaft-like conformation without severe restrictions from the neighboring *sn*-1 acyl chain. This set of ($\delta_1' = -140°$, $\delta_2' = -65°$)-torsion angles is thus taken as the initial crude or "guesstimate" atomic coordinates for our subsequent MM calculations in determining the refined structure and the minimized energy of the kink-forming sequence Δtg^-. The refinements of various kink-forming sequences are discussed in a later section. It should be noted at this point, however, that the guessed δ_1'-angle of −140° is more of a *skew* (*s*) bond than a *trans* bond; hence, we designate the derived kink-forming sequence as the sequence Δs^-g^-. In fact, the sequence Δs^-g^- with a set of ($\delta_1' = -140$, $\delta_2' = -65°$)-torsion angles is virtually identical to the kink-forming sequence first proposed for an unsaturated hydrocarbon chain back in 1977 (Huang, 1977; Lagaley et al., 1977). Consequently, we denote the kink generated by the sequence Δs^-g^- as the Type Ia or Δs^-g^- kink.

In the process of deriving Type Ia Δ-containing kink, or the Δs^-g^- kink, the first step is to assume that the *gauche*$^+$ bond in the template sequence g^+tg^- is conformationally similar to a *cis* carbon-carbon double bond (Δ), and from which a sequence Δtg^- is constructed as a precursor of a possible kink. This process is summarized in Fig. 6 *a–c*. The general protocol developed here in identifying the Type Ia kink is also adopted to derive other types of kinks for POPC. Fig. 6, *a*, *b*, and *d* depict an example in which the process involved in generating a $s^+\Delta tg^-$ kink is stepwise illustrated as constructed with computer graphics. Fig. 6 *a* shows the model structure of POPC having an all-*trans* *sn*-1 acyl chain and a *sn*-2 acyl chain with the sequence $t\Delta tt$ around the Δ-bond. This is a view in which the zigzag plane of the *sn*-1 acyl chain is topologically oriented to lie on the X-Y (or the paper) plane. Fig. 6 *b* shows the same molecule after the C(11)-C(12) carbon-carbon single bond in the *sn*-2 acyl chain has undergone a *trans*→*gauche*$^-$ rotational isomerization. The generation of such a structure is based on the assumption that the conformation of an unsaturated hydrocarbon chain with a sequence $t\Delta tg^-$ may roughly approximate the topology of a corresponding saturated hydrocarbon chain with a kink sequence of tg^+tg^-. Fig. 6 *b* indeed shows that the rotation of the C(11)-C(12) bond to a g^- conformation with a δ_2' value of −65° results in an upward movement of the lower linear segment of the *sn*-2 acyl chain. Moreover, this movement also causes the zigzag plane of the lower linear segment of the *sn*-2 acyl chain to lie on the X-Y plane. The next step involves the adjustment of the δ_1-angle so that the sequence $t\Delta tg^-$ is substituted by the sequence $s^+\Delta tg^-$. This substituted sequence with a set of guessed ($\delta_1 = +140°$, $\delta_2' = -65°$)-torsion angles transforms the *sn*-2 acyl chain into a crankshaft-like topology as shown in Fig. 6 *d*. The kink in this secondary structural element, called Type IIa or $s^+\Delta tg^-$ kink, differs principally from Type Ia or Δs^-g^- kink in that the torsion angle of the carbon-carbon single bond immediately preceding, not succeeding, the Δ-bond has been adjusted as shown in Fig. 6 *d*.

If both the carbon-carbon single bonds adjacent to the Δ-bond are adjusted, two additional kink-forming-sequences can be generated as shown in Fig. 6 *e* and *f*. Similar to Type Ia and IIa kink- forming sequences, these sequences $s^-\Delta s^-g^-$

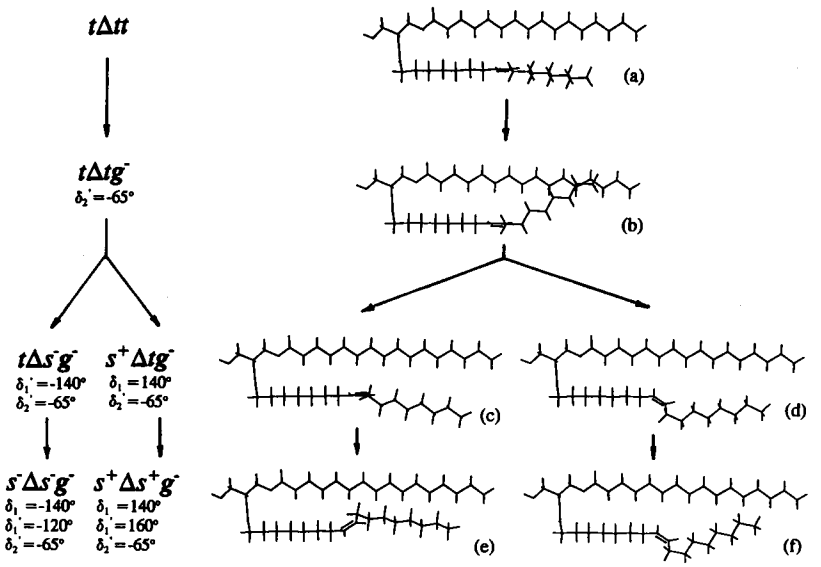

FIGURE 6 Four different types of the secondary structural element arising from a common precursor sequence. The pathways from which the four kink-forming sequences are being generated from a common sequence are shown on the left, and their corresponding structures are shown on the right.

and $s^+\Delta s^+g^+$ are progressively derived from the sequence $t\Delta tt$ in the *sn*-2 acyl chain of POPC via a common precursor sequence $t\Delta tg^-$. The molecular motifs generated by the sequences $s^-\Delta s^-g^-$ and $s^+\Delta s^+g^-$ are called Type Ib ($s^-\Delta s^-g^-$) and IIb ($s^+\Delta s^+g^-$) kinks, respectively. All together, these four deduced kinks shown in Fig. 6 belong to Group I secondary structural elements; hence, they are also named Group I kinks. It should be emphasized that the various successive steps formulated in Fig. 6 represent only the logical processes with which Type I and Type II kinks may be derived individually from a common precursor sequence. They do not imply the actual pathways from which the various types of crankshaft-like kinks may be generated in the lipid bilayer.

Once Group I kinks are set on stage, other groups of crankshaft-like kink can be derived in a similar manner using a different common precursor sequence for each of the other groups as illustrated in Fig. 7. For instance, the common precursor sequences for Group II and Group IV kinks are $g^+t\Delta t$ and $g^-t\Delta t$, respectively. They are derived on the basis that a Δ-bond may substitute a g^- bond and a g^+ bond in the template sequences g^+tg^- and g^-tg^+, respectively. Likewise, after substituting a g^- bond by a Δ-bond in a template sequence of g^-tg^+, the resulting sequence $t\Delta tg^+$ is subsequently used as a common precursor to derive Group III kinks.

In all of the derived sequences shown in Fig. 7, initial guesses must be made about the values of $\pm\delta_1(\delta_1')$- and $\pm\delta_2(\delta_2')$-angles. Potential energy contour maps (Fig. 4 *A–C*) together with computer graphics are served as a combined guide in finding the guessed values of δ_1 (or δ_1', usually $\pm140°$ or $\pm120°$), whereas the δ_2 (or δ_2')-angle is kept at a fixed value (usually at or near a local minimum of $\pm65°$). These initial guessed values are presented in Table 1.

Energy-minimized conformations of Δ-containing kinks in the diglyceride moiety of POPCs

With the combination of molecular mechanics calculations and computer graphics, each of the refined conformations of Group I to Group IV kinks in the *sn*-2 acyl chain of POPC can be obtained individually and recognized visually. Specifically, the refinement of the diglyceride moiety of POPCs with guessed torsion angles (given in Table 1) has been carried out with the MM2 force field method using the Version 85 program. The torsion angles of all the refined structures together with their steric energies are presented in Table 1 under the guessed values. Here, the minimal energy conformation of the diglyceride moiety of the mixed-chain lipid with a given kink sequence in the *sn*-2 acyl chain is taken as the computationally refined structure of POPC containing that particular sequence.

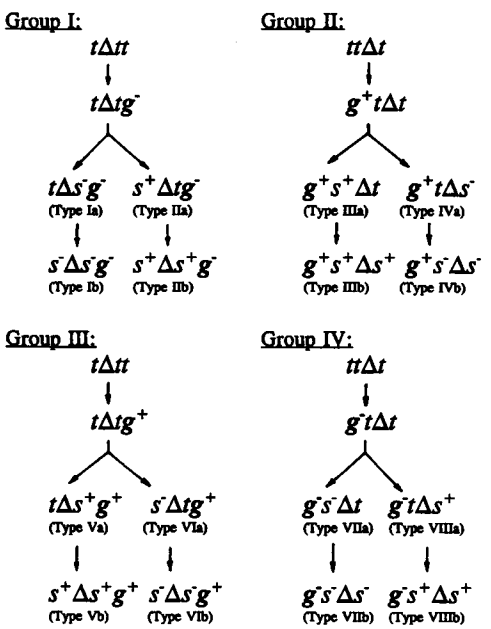

FIGURE 7 The four basic groups of secondary structural elements derived for the *sn*-2 acyl chains of POPC. Within each group, four types of the secondary structural element can arise from a common precursor sequence.

TABLE 1 The various kink models and their crude estimated and energy-minimized torsion angles as detected in the *sn*-2 acyl chain of 1-palmitoyl-2-oleoyl-phosphatidylcholine

Group	Type	Sequence	CEV* EMV*	δ_2	δ_1	Δ (degrees)	δ_1'	δ_2'	E_s (kcal/mol)
I	Ia	$t\Delta s^- g^-$	CEV	180	180	0	−140	−65	
			EMV	176.0	−174.5	−0.6	−139.9	−73.1	22.8
	Ib	$s^-\Delta s^- g^-$	CEV	180	−140	0	−120	−65	
			EMV	177.0	−168.7	−0.4	−139.0	−73.1	22.9
	IIa	$s^+\Delta t g^-$	CEV	180	140	0	180	−65	
			EMV	176.4	134.1	0.4	176.8	−65.0	24.3
	IIb	$s^+\Delta s^+ g^-$	CEV	180	135	0	160	−65	
			EMV	177.1	133.4	0.4	155.6	−66.3	24.5
II	IIIa	$g^+ s^+\Delta t$	CEV	65	140	0	180	180	
			EMV	66.8	141.4	0.2	173.5	178.9	23.2
	IIIb	$g^+ s^+\Delta s^+$	CEV	65	130	0	140	180	
			EMV	66.2	134.0	−0.4	153.8	176.6	22.8
	IVa	$g^+ t\Delta s^-$	CEV	65	180	0	−120	180	
			EMV	64.1	173.0	0.5	−107.9	−177.0	22.8
	IVb	$g^+ s^-\Delta s^-$	CEV	65	−165	0	−120	180	
			EMV	64.6	172.4	0.7	−110.1	−176.2	22.8
III	Va	$t\Delta s^+ g^+$	CEV	180	180	0	140	65	
			EMV	177.6	169.1	0.0	141.9	67.1	23.1
	Vb	$s^+\Delta s^+ g^+$	CEV	180	140	0	120	65	
			EMV	178.9	149.4	0.3	116.0	68.2	23.1
	VIa	$s^-\Delta t g^+$	CEV	180	−140	0	180	65	
			EMV	176.5	−132.3	0.1	173.9	70.6	25.5
	VIb	$s^-\Delta s^- g^+$	CEV	−180	−140	0	−165	65	
			EMV	171.4	−139.2	−0.9	−173.7	62.9	25.5
IV	VIIa	$g^- s^-\Delta t$	CEV	−65	−140	0	180	180	
			EMV	−75	−147.9	−0.1	−178.5	178.5	24.2
	VIIb	$g^- s^-\Delta s^-$	CEV	−69	−130	0	−130	180	
			EMV	−72.5	−124.7	0.4	−117.5	−175.8	23.9
	VIIIa	$g^- t\Delta s^+$	CEV	−65	180	0	120	180	
			EMV	−65.2	−175.5	0.8	117.5	−177.5	23.5
	VIIIb	$g^- s^+\Delta s^+$	CEV	−65	180	0	140	180	
			EMV	−64.2	152.7	0.5	99.0	173.8	23.5
Crystal oleate‡		$g^+ s^+\Delta s^+$	CEV	70	123	0	127	180	
			EMV	68.5	131.8	−0.2	155.6	177.6	23.1

* CEV and EMV denote, respectively, the crude estimated and energy-minimized values of various torsion angles (δ_2, δ_1, Δ, δ_1', δ_2') as defined in Fig. 1 *A*.

‡ The torsion angles given in CEV are taken from the crystallographic data of an oleate chain obtained with cholesteryl oleate in single crystals at 123 K (Gao and Craven, 1986).

After energy minimizations, computer graphics-illustrated structures of POPCs with Group I kinks are presented in Fig. 8 (uppermost row). It is evident from Fig. 8, *A* and *B* that the mixed-chain lipid molecules containing Type Ia and Ib kinks are indistinguishable. In fact, all the torsion angles around the Δ-bond for these two types of kinks are virtually identical (Table 1), indicating that they are degenerate or intrinsically of the same kind, not allowing any visual distinction. In each energy-minimized structure, the flat six-atom structural unit and the zigzag plane of the upper segment of the *sn*-2 acyl chain are coplanar, and the two C-H bonds of the olefinic carbons, on the X-Y (or the paper) plane, point toward the viewer. It is interesting to note that the olefinic C(9) and C(10) atoms are 3.87 and 3.70 Å, respectively, away from C(6) atom in the *sn*-1 acyl chain. Moreover, C(11), C(13), C(15), and C(17) atoms of the *sn*-2 acyl chain fit optimally into the centers of the V-shaped grooves formed by C(6)-C(8), C(8)-C(10), C(10)-C(12), and C(12)-C(14) atoms, respectively, of the adjacent *sn*-1 acyl chain with an averaged interatomic distance of 3.89 Å. The steric complementarity of the van der Waals contact surfaces makes a major contribution to the overall stability of POPC with Type Ia and Ib kinks.

The computationally refined conformations of POPCs with Type IIa and IIb kinks are similar (Fig. 8, *C* and *D*), but they are distinctively different from those with Type Ia and Ib kinks. The planar six-atom structural unit in each Type II kink is canted on the X-Y plane with the C(10)-end tilting downward and the C(10)-H bond pointing somewhat outward from the X-Y plane. This tilt is a bit more pronounced for Type IIb kink, giving the lower segment of the *sn*-2 acyl chain an overall wider separation distance from the adjacent *sn*-1 acyl chain. For instance, C(11) atom of the *sn*-2 acyl chain is 5.29 Å away from C(6) atom of the *sn*-1 acyl chain for Type IIa kink, and the same separation distance is increased to 5.56 Å for Type IIb kink.

Detailed MM calculations in combination with computer graphics led to the deduction of the refined structures of the diglyceride moieties of POPCs with Group II kinks when the appropriate guessed torsion angles shown in Table 1 were used. The results, illustrated in Fig. 8 *E–H*, indicate that two particularly instructive features are common to all of the

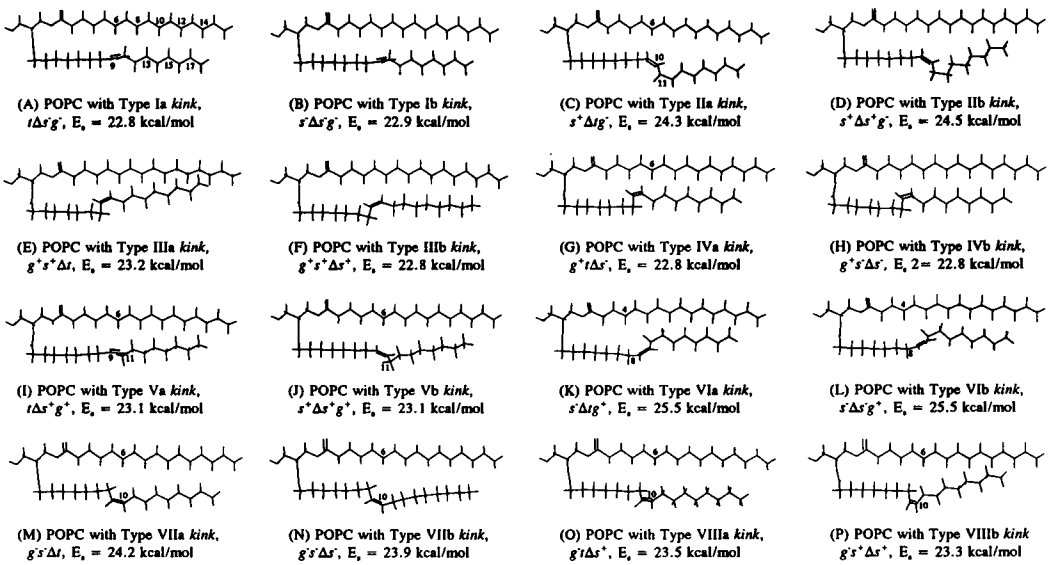

FIGURE 8 The minimum energy structures of the diglyceride moieties of POPC with Groups I–IV secondary structural elements. These structures are constructed based on the refined values of torsion angles given in Table 1, derived for POPC with various kink-forming sequences.

refined kinks: (1) the lower segment of the *sn*-2 acyl chain lies in between the *sn*-1 acyl chain and the upper segment of the *sn*-2 acyl chain; (2) each flat six-atom structural unit is canted on the X-Y plane with C(10)-end of the flat plane tipping upward and the C(10)-H bond pointing away from the viewer. This latter feature appears to steer specifically the lower linear segment of the *sn*-2 acyl chain to pack closer against the adjacent *sn*-1 acyl chain, resulting in an energetically favored van der Waals contact interaction between the *sn*-1 and the *sn*-2 acyl chains.

In the case of Type IIIa (or $g^{+}s^{+}\Delta t$) kink, the lower segment of the *sn*-2 acyl chain crosses the axis of the *sn*-1 acyl chains at the methyl terminus (Fig. 8 *E*). This intersecting-axis geometry, however, is eliminated in Type IIIb (or $g^{+}s^{+}\Delta s^{+}$) kink. Instead, the zigzag planes of the two acyl chains are nearly perpendicular to each other (Fig. 8 *F*). Type IVa (or $g^{+}t\Delta s^{-}$) and IVb (or $g^{+}s^{-}\Delta s^{-}$) kinks are degenerate (Fig. 8, *G* and *H*). The lower segments of the *sn*-2 acyl chain and the *sn*-1 acyl chain are in the closest van der Waals contact; interestingly, the even-carbon atoms of the lower *sn*-2 acyl chain protrude perfectly into the V-shaped grooves of the *sn*-1 acyl chain, and the even-carbon atoms of the *sn*-1 acyl chain starting from C(6) atom are, in turn, inserted optimally into the V-shaped grooves of the *sn*-2 acyl chain with an averaged interatomic distance of 3.85 Å. This geometric complementarity produces a tight intramolecular chain-chain packing, resulting in one of the smallest steric energies of 22.8 kcal/mol for all the energy-minimized structures examined (Table 1).

The computationally refined structures of various Group III kinks in the glyceride moieties of POPCs are shown in Fig. 8 (second row from the bottom). A central feature of Type Va (or $\Delta s^{+}g^{+}$) kink is that the large deviations in torsion angles from 180° occur in those carbon-carbon single bonds succeeding the Δ-bond. It is thus anticipated that, on the X-Y plane, the six-atom structural unit and the zigzag plane of the upper linear segment of the *sn*-2 acyl chain are most likely to be coplanar and that the olefinic C(9)-H bond projects outward at the viewer. These predicted structural features, reminiscent of those encountered in Type Ia kink, are by and large observed in the refined Type Va kink as shown in Fig. 8 *I*, except that the flat six-atom structural unit is a bit tilted. Consequently, the lower segment of the *sn*-2 acyl chain is packed against the adjacent *sn*-1 acyl chain at a somewhat wider separation distance in comparison with Type Ia kink. For instance, the interatomic distance between C(11) atom of the *sn*-2 acyl chain and C(6) atom of the *sn*-1 acyl chain is 4.39 Å, whereas the separation distance between the same pair of carbon atoms in Type Ia kink is 3.91 Å.

The minimum-energy conformation of Type Vb (or $s^{+}\Delta s^{+}g^{+}$) kink is illustrated in Fig. 8 *J*. In contrast to Type Va kink, the lower segment of the *sn*-2 acyl chain in Type Vb kink is a bit more tilted; consequently, the chain axis of the lower segment of the *sn*-2 acyl chain and the long chain axis of the *sn*-1 acyl chain are no longer parallel to each other. In addition, the sequence $s^{+}\Delta s^{+}g^{+}$ places the zigzag plane of the lower segment of the *sn*-2 acyl chain approximately perpendicular to the zigzag plane of the *sn*-1 acyl chain rather than parallel as seen in Type Va kink.

The refined structures of Type VIa (or $s^{-}\Delta tg^{+}$) and Type VIb (or $s^{-}\Delta s^{-}g^{+}$) kinks are strikingly similar as shown in Fig. 8, *K* and *L*. The degeneracy of the two kinks is evident from their torsion angles and steric energies given in Table 1. Each six-atom structural unit is tilted with the C(10)-end tipping upward against the adjacent *sn*-1 acyl chain and the C(9)-H bond, on the X-Y plane, pointing toward the viewer. The most unusual feature shared by Type VIa and VIb kinks is that the upper segment of the *sn*-2 acyl chain and the initial segment of the adjacent *sn*-1 acyl chain are at a separation distance considerably greater than the sum of van der Waals

radii of groups involved. For instance, C(4) atom of the *sn*-1 acyl chain and C(8) atom of the *sn*-2 acyl chain in Type VIa and VIb kinks are separated by 4.75 and 4.50 Å, respectively. In contrast, a separation distance of 3.82 Å is found between the same pair of nonbonded carbons in the refined structure of POPC-containing type Va kink (Fig. 8 *I*). For this reason, the chain-chain van der Waals attractive force is relatively weak in the upper region of the mixed-chain lipid with Type VIa or Type VIb kink.

Fig. 8 *M–P* illustrate the fourth group of secondary structural elements consisting of energy-minimized structures of Type VIIa, VIIb, VIIIa, and VIIIb kinks, respectively. These four deduced structures share a common distinctive feature: each flat six-atom structural unit is tilted somewhat on the X-Y plane from the upper-left to the lower-right, with the two C-H bonds typically pointing downward. This common topology makes the planar six-atom structural unit appear as a convex bulge. This bulge is most accentuated in Type VIIb (or $g^-s^-\Delta s^-$) kink, in which the olefinic C(10) atom is 5.42 Å away from C(6) atom of the *sn*-1 acyl chain. The separation distances of the same nonbonded carbon-carbon pairs are 5.16, 5.06, and 5.36 Å in Type VIIa, VIIIa, and VIIIb kinks, respectively. Although the prominent bulge in the *sn*-2 acyl chain with Type VIIb kink can diminish considerably the van der Waals attractive force between the six-atom structural unit and the *sn*-1 acyl chain, the mutually perpendicular orientation of the *sn*-1 and *sn*-2 acyl chains compensates the energy loss somewhat; consequently, the overall steric energy of the diglyceride moiety of POPC with Type VIIb kink (23.9 kcal/mol) is in between those calculated for Type VIIa (24.2 kcal/mol) and Type IIIb (23.3 kcal/mol) kinks.

Overall, Fig. 8 shows 16 molecular rotomers for POPC. Conformational degeneracies are detected for pairs of (Type Ia, Type Ib), (Type IVa, Type IVb), and (Type VIa, Type VIb). It should be mentioned that each of the remaining 13 molecular rotomers should not be considered as a distinct, rigid species. In fact, variations in torsion angles of $\pm 5°$ are not uncommon within each type of the 13 crankshaft-like kinks due to the great flexibility of δ_1- and δ_1'-angles in the *sn*-2 acyl chain. These variations may result in energy-minimized structures with E_s values slightly greater than (≤ 1 kcal/mol) those E_s values shown in Table 1. It should be emphasize that the *sn*-1 acyl chain in each of the 16 rotomers is in an all-*trans* conformation, reflecting that these rotomers are in the gel state ($T < T_m$).

Comparison of oleate chain conformation in cholesteryl oleate crystals with the calculated oleate chain conformation in POPC

Unfortunately, no x-ray single-crystal structural analysis of any mixed-chain phospholipid with an unsaturated *sn*-2 acyl chain has yet been done; consequently, the various kink models deduced by computer-based modeling method as developed in this study cannot be confirmed definitively by experimental data. However, the structural data of an oleate chain obtained with cholesteryl oleate at 123 K in single crystals are available (Gao and Craven, 1986); these crystallographic data can provide insights into the molecular structure of POPC packed in the highly ordered lipid bilayer at $T < T_m$. Moreover, these structural data can be used indirectly to test, but not to prove, the validity of our deduced kink models.

Molecular mechanics together with computer graphics can provide information about the conformational difference in oleate chain between cholesteryl oleate and POPC. Specifically, molecular conformation of oleate chain established by crystallographic data of cholesteryl oleate can be used as starting geometry for the *sn*-2 acyl chain of POPC. This structure containing the oleate chain of cholesteryl oleate is thus first constructed. Energy minimization of this constructed structure is subsequently carried out. The *sn*-2 acyl chain of the resulting structure can then be compared with those containing various kink motifs developed for POPC as shown in Fig. 8. This comparison is regarded as an indirect test of the topology of the kink models developed in this study.

Fig. 9 *A* shows the starting geometry of POPC constructed on the basis of torsion angles for oleate chain in crystalline cholesteryl oleate (Table 1) obtained at 123 K as reported by Gao and Craven (1986). The planar six-atom structural unit is seen to tilt upward with its C(10)-end directing toward the *sn*-1 acyl chain, the lower zigzag segment of the *sn*-2 acyl chain being perpendicular to the zigzag plane of the *sn*-1 acyl chain. The interatomic distance between olefinic C(10) atom and C(6) atom of the *sn*-1 acyl chain is so short (1.96 Å) that this initially constructed structure is sterically improbable. It is thus anticipated that because of interchain overcrowding the *sn*-1 acyl chain will force some adjustments of δ_1- and δ_1'-angles, sufficient to move the lower segment of the *sn*-2 acyl chain to a nearby position of favorable interaction, during the refinement process of energy minimization. The refined structure is shown in Fig. 9 *B*, and the modified values of torsion angles for the refined structure together with the steric energy are summarized in Table 1 (bottom row). In this computationally refined structure, the *sn*-1 acyl chain makes many van der Waals contacts with the *sn*-2 acyl chain. For example, the interatomic distance between olefinic C(10) atom and C(6) atom of the *sn*-1 acyl chain is increased to 3.62 Å, a favorable van der Waals interaction distance. Concomitantly, the apparent chain length of the *sn*-2 acyl chain is increased slightly from 19.26 to 19.50 Å. These structural rearrangements provide valuable information for understanding the influence of the all-*trans* *sn*-1 acyl chain on the formation of an appropriate kink along the *sn*-2 acyl chain in a mixed-chain lipid. Most interestingly, this computationally refined structure is remarkably similar to POPC with Type IIIb kink (Figs. 8 *F* and 9 *C*) developed in earlier sections. In fact, the largest difference in torsion angle between these two structures is only 2.3° for δ_1-angle (Table 1). This striking similarity is unlikely to be a mere coincidence. Instead, it can be taken as strong evidence arguing in favor of the validity of our molecular modeling approach to identify

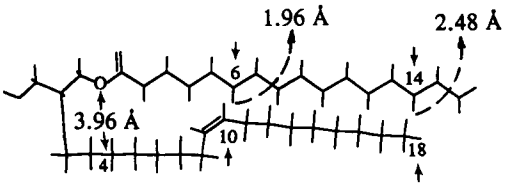

(A) POPC with torsion angles of the oleate chain in cholesteryl oleate (Gao and Craven, 1986)

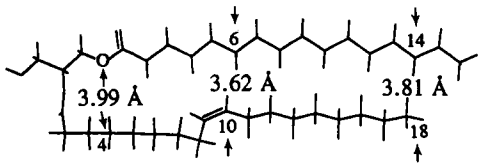

(B) Energy-minimized structure of (A)

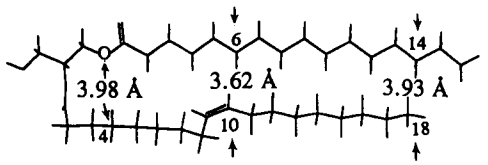

(C) POPC with Type IIIb *kink*

FIGURE 9 (*A*) Deduced POPC structure in which the *sn*-2 acyl chain has the same conformation as the oleate chain of crystal cholesteryl oleate established by x-ray crystallography. The chain-chain separation distance is sterically disallowed in this case. (*B*) The energy-minimized structure of *A*. The juxtaposition of the two acyl chains is clearly seen to be sterically optimized. (*C*) POPC with Type IIIb kink. This deduced lipid structure has an overall conformation that is indistinguishable from that of the energy-minimized POPC structure derived from the oleate chain of cholesteryl oleate as shown in *B*.

and to characterize Δ-containing kink models for mixed-chain phospholipids at $T < T_m$. It should be stated that the x-ray study of Gao and Craven results in a single structure of oleate chain at 123 K with regard to molecular conformations. However, many different conformations of oleate chain may exist at higher temperatures for cholesteryl esters. The 16 rotormers presented in Fig. 8 for POPC are suggested for the lipid species packed in the highly ordered gel state of the lipid bilayer. Because the T_m value of the lipid bilayer comprised of POPCs is −2.6°C (Huang, 1991), these rotormers are thus suggested to exist at temperatures below −2.6°C.

Packing geometries of tetrameric POPCs

In the foregoing section, one piece of structural evidence is presented to demonstrate the validity of molecular modeling approach in deriving the secondary structural motif of the unsaturated *sn*-2 acyl chain in a monomeric POPC at $T < T_m$. All together, we have derived four possible groups of Δ-containing kinks, and the structure of each member of these four groups is illustrated in Fig. 8. In this section, we extend this work and to use monomeric POPCs with various types of kink motif as bases to construct multiple tetramers of POPCs. This assembly of multiple tetramers is viewed, to a first approximation, as a simple model for the gel-state lipid bilayer. Specifically, we attempt to seek answers to the following two questions. (1) To what extent will the conformation of a Δ-containing kink exhibited by a monomer be retained in the lipid assembly? (2) As the multiple tetramers of mixed-chain lipid are assembled, the maximum binding (or stabilization) energy of the assembly occurs when the overall contact surface among the monomers is maximal. Within a defined geometric or lattice arrangement of the monomers, the overall contact surface among monomers depends on the structure of the constituent monomeric species. For instance, if there are constraints between the monomers due to the presence of a specific type of Δ-containing kink, these constraints will be reflected in the stabilization energy of the assembly. We are interested to learn what is the averaged stabilization energy of the lipid bilayer contributed by the constituent monomeric species containing a defined type of kink? Towards these ends, we have carried out a systematic study of the lipid assembly as described in the following paragraphs.

In this study, we have first selected a representative kink from each of the four groups shown in Figs. 7 and 8. Two POPC molecules, each containing the same selected kink, are arranged to form a partially interdigitated *trans*-bilayer dimer according to the method described previously (Li et al., 1993). After energy minimization, the dimers are consolidated to form two types of tetramer: the front-to-back (F-B) and the up-and-down (U-D) tetramers. In the F-B type, two *trans*-bilayer dimers are staggered in the front-to-back arrangement; in the U-D type, two *trans*-bilayer dimers are aligned side-by-side and lie on a common plane (Li et al., 1993). These tetrameric structures are subjected to energy minimization, and their steric energies are recorded.

The energy-minimized structures of tetrameric POPCs with Type Ia kink packed in the front-to-back (F-B) and up-and-down (U-D) arrangements are shown in Fig. 10, *A* and *B*, respectively. The values of torsion angles for various bonds in the vicinity of the Δ-bond for these two forms of tetramer are summarized in Table 2. The steric energy for each of the tetramers is given under the corresponding computer-generated illustration shown in Fig. 10 as well as in Table 2. Interestingly, the torsion angles for Type Ia kink in the two forms of tetramer are only slightly different from those in the monomer (Table 2). In this case, the largest deviation occurs at the δ_2'-angle between the monomer and one of the component monomers of the F-B tetramer, corresponding to a 8° reorientation of the C(11)-C(12) single bond in the *sn*-2 acyl chain in the F-B tetramer. These computational results thus indicate that the overall conformation of the Δ-containing kink derived for monomeric POPC is essentially retained in the tetramer. However, fine turnings

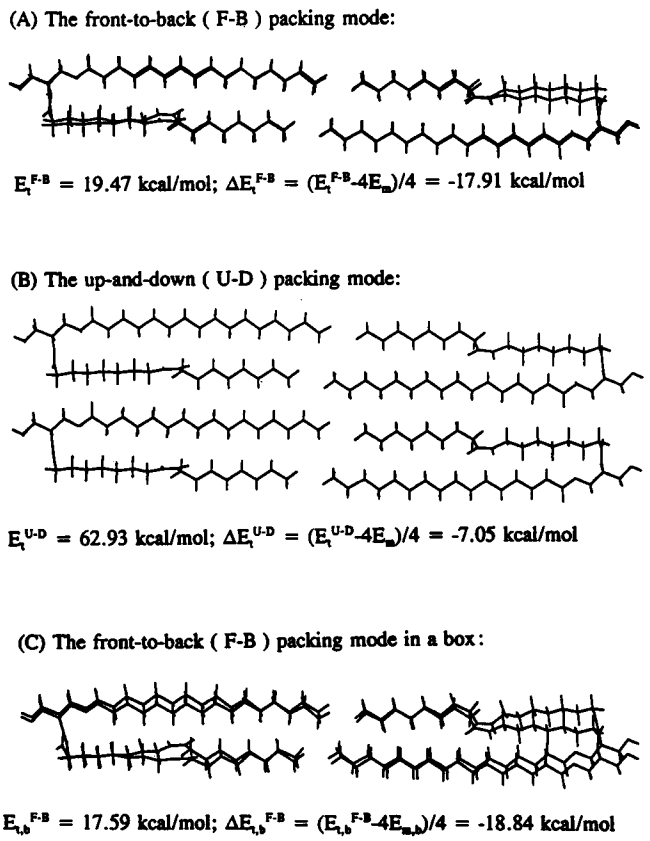

FIGURE 10 The computer-generated figures for the energy-minimized structures of the tetrameric POPC containing Type Ia kink. (*A*) Two pairs of *trans*-bilayer dimers are arranged in a front-to-back packing mode. (*B*) Two pairs of *trans*-bilayer dimers are arranged in an up-and-down packing mode. (*C*) A tetramer model obtained by periodic boundary conditions. For comparison purposes, the rectangular box is removed from this figure.

in the δ_1- and δ_1'-torsion angles are always accompanied with the monomer→tetramer aggregation.

With MM2 program, the steric energies of the F-B and U-D tetramers for POPCs with Type Ia kink are calculated to be 19.47 and 62.93 kcal/mol, respectively. The steric energy of the most stabe monomer (E_m) is 22.78 kcal/mol. The smaller E_t^{F-B} value of 19.47 kcal/mol for the F-B tetramer indicates that the aggregate is stabilized strongly by the favorable intermolecular interactions among the monomers in the front-to-back packing mode. The stabilization energy of the F-B tetramer contributed by the monomer can be calculated as follows: $\Delta E_t^{F-B} = (E_t^{F-B} - 4E_m)/4 = -17.91$ kcal/mol. Similarly, the stabilization energy of the U-D tetramer contributed by each monomer is obtained as $\Delta E_t^{U-D} = (E_t^{U-D} - 4E_m)/4 = -7.05$ kcal/mol. This smaller negative value can be attributed primarily to the smaller contact surface among monomers in the tetramer with a U-D packing mode. The overall averaged stabilization energy for the tetramer contributed by the monomer ($\sum \Delta E_t^{AVE}$) is the sum of ΔE_t^{F-D} and ΔE_t^{U-D} divided by 2, and this value is −12.48 kcal/mol for the tetramer of POPC with Type Ia kink.

The overall averaged stabilization energies for POPCs with representative kinks from other groups as contributed by their constituent monomeric species are also calculated, and the results are summarized in Table 3. Of the four species studied, the values of $\sum \Delta E_t^{AVE}$ varies from −11.56 kcal/mol for Type Vb kink to −13.05 kcal/mol for Type VIIIa kink, indicating that the energetic differences among the various kinks in the tetramer are not significantly different. These small energy differences can be used to estimate the relative populations of these various species in the lipid assembly, if the entropy contribution, to a first approximation, is ignored. For instance, if the $(-\sum \Delta E_t^{AVE})$ value of 13.05 kcal/mol calculated for the mixed-chain lipid having Type VIIIa (or $g^-t\Delta s^+$) kink is taken as the reference state, the relative populations, at 25°C, of the four lipid species listed in Table 3 can be readily obtained using the Boltzmann distribution and conservation of mass laws as follows: Type Ia kink, 15.26%; Type IIIb, 33.55%; Type Vb, 2.87%; Type VIIIa, 48.32%. This simple estimation serves to demonstrate that the four groups of Δ-containing kinks derived in this study can all be present in appreciable quantities, at −10°C, in the gel-state lipid bilayer consisting of mixed-chain phospholipids with Δ-bonds. For comparison, the averaged stabilized energy of the lipid bilayer contributed by a saturated mixed-chain lipid species, and the same energy contributed by its rotamer with a g^+tg^- kink at the center of the *sn*-2 acyl chain are also listed in Table 3. The relative populations of the saturated lipids with and without the g^+tg^- kink in the bilayer at −10°C can be calculated to be 0.02% and 99.98%, respectively, indicating that the amount of the saturated lipid with the g^+tg^- kink is extremely low in the gel-state lipid bilayer composed of only saturated phospholipids.

Multiple tetramers simulated by periodic boundary conditions

To check the validity of our averaged tetramer model as a reasonable starting bilayer structure, an energy-minimized assembly of tetrameric POPCs arranged in the front-to-back motif is first placed in a rectangular box (35.0 × 30.8 × 56.1 Å) in which the front-to-back interface between the two superimposed *trans*-bilayer dimers lie in parallel to the Y-Z plane of the box, and the long molecular axis is aligned along the Z-axis. Three-dimensional periodic boundaries are then employed to simulate the mutiple lipid-lipid interactions in a large continuous system in which the original rectangular box is surrounded by 26 identical replicas of image boxes. Thus, the tetramer in the original box is periodically replicated in all directions. Specifically, the F-B tetramer is in the central cavity of three layers of rectangular boxes (3^3-1) in a three-dimensional space. Consequently, each lipid molecular in the original rectangular box is surrounded by six neighboring lipid molecules in the two-dimensional plane of the lipid bilayer. The large system is then energy-minimized using the MM$^+$ program in HyperChem. The various energy terms for the energy-minimized POPC as a monomer ($E_{m,b}$) and as a tetramer in a large system with 26 neighboring boxes ($E_{t,b}^{F-B}$) as calculated by the MM$^+$ program in HyperChem are recorded.

TABLE 2 Comparisons of the torsion angles for POPC (with Type Ia kink) in the monomer with those in the tetramers

Lipid	Packing mode*	Sequence	δ_2 (deg)	δ_1 (deg)	Δ (deg)	δ_1' (deg)	δ_2' (deg)	E_s (kcal/mol)
POPC	monomer	$t\Delta s^- g^-$	176.0	−174.5	−0.6	−139.9	−73.1	22.83
POPC	F-B	$t\Delta s^- g^-$	179.3	−173.9	−0.1	−143.3	−81.5	19.47
POPC	U-D	$t\Delta s^- g^-$	175.6	−174.3	−1.1	−142.0	−76.7	62.93
POPC	F-B,Box	$t\Delta s^- g^-$	168.2	174.2	−2.2	−134.6	−71.4	17.59

* F-B and U-D represent the front-to-back and up-and-down packing modes, respectively, of the tetramers, as illustrated in Fig. 10, *A* and *B*, respectively, for 1-palmitoyl-2-oleoyl-phosphatidylcholine (POPC) molecules. F-B,Box represents the tetramer in a box surrounded by 26-image neighboring boxes.

TABLE 3 Stabilization energies of tetrameric POPC containing different types of kink and of tetrameric C(16):C(18)PC* with and without a g^+tg^- kink

Lipid	Sequence	E_m‡	E_d	$E_t^{F\text{-}B}$	$E_t^{U\text{-}D}$	$-\Delta E_t^{F\text{-}B}$	$-\Delta E_t^{U\text{-}D}$	$-\sum \Delta E_t^{AVE}$	RP§ (%)	$E_{m,b}$	$E_{t,b}^{F\text{-}B}$	$-\Delta E_{t,b}^{F\text{-}B}$
POPC	$t\Delta s^- g^-$	22.83	43.37	19.47	62.93	17.91	7.05	12.48	15.26	23.29	17.59	18.84
POPC	$g^+s^+\Delta s^+$	22.78	43.05	20.67	58.68	17.61	8.11	12.86	33.55	23.24	17.17	18.95
POPC	$s^+\Delta s^+ g^+$	23.14	43.37	23.20	66.44	16.98	6.17	11.56	2.87	23.59	24.45	17.13
POPC	$g^- t\Delta s^+$	23.48	43.84	16.61	61.24	18.63	7.47	13.05	48.32	23.88	13.64	19.84
C(16):C(18)PC	all *trans*	20.15	37.91	1.99	49.13	19.66	7.87	13.76	99.98	20.61	−2.96	21.35
C(16):C(18)PC	$g_9^+ t_{10} g_{11}^-$	23.32	44.07	22.19	64.80	17.79	7.12	12.45	0.02	23.76	17.43	19.40

* C(16):C(18)PC. A saturated mixed-chain phospholipid, 1-palmitoyl-2-steroyl-phosphatidylcholine.

‡ The unit for all energy terms (E) is kcal/mol. E_m, E_d, and E_t are steric energies for the monomeric, *trans*-bilayer dimeric, and tetrameric phospholipids, respectively, calculated from MM2(85) program of Allinger. $E_{m,b}$ is the steric energy of monomeric phospholipids calculated from MM^+ in HyperChem. The superscripts F-B and U-D denote the front-to-back and up-and-down packing models, respectively; the subscript b represents the results obtained from periodic boundary conditions; see text and Fig. 10 for the definitions of F-B and U-D packing modes. In calculations of the various ΔE values in columns 7–9 for POPC, the minimum E_m value of 22.78 kcal/mol was used throughout for all four sequences. In calculating the last column, however, the $E_{m,b}$ of 23.24 kcal/mol was used for the four sequences of POPC.

§ RP is the relative population calculated from $\sum \Delta E_t^{AVE}$.

The calculated energy terms ($E_{m,b}^{F\text{-}B}$ and $E_{t,b}^{F\text{-}B}$) for POPCs with representative kinks from the four groups shown in Fig. 8 together with the energy terms for saturated 1-palmitoyl-2-stearoyl-phosphatidylcholine and its rotomer with a g^+tg^- kink at the center of the *sn*-2 acyl chain are presented in Table 3. In addition, the stabilization energy of the F-B tetramer in the large system with 26 neighboring boxes contributed by the monomer, $-\Delta E_{t,b}^{F\text{-}B}$, for each lipid species is also calculated and the results are also given in Table 3.

Clearly, the calculated values of the energy terms of $-\Delta E_{t,b}^{F\text{-}B}$ and $-\sum \Delta E_t^{AVE}$ for the four rotomers of POPC shown in Table 3 are different; however, these two sets of data are parallel. Consequently, conclusions concerning the mutiple lipid-lipid interactions drawn from either the averaged tetramer model ($-\sum \Delta E_t^{AVE}$) or the tetramer in a larger system with 26 neighboring boxes ($\Delta E_{t,b}^{F\text{-}B}$) are comparable, suggesting that the averaged tetramer model is a reasonable simple model for the gel-state lipid bilayer. It should be noted that only the values of $-\sum \Delta E_t^{AVE}$ and $-\Delta E_{t,b}^{F\text{-}B}$ are parallel. Other values such as $\Delta E_t^{F\text{-}B}$ and $\Delta E_t^{U\text{-}D}$ shown in Table 3 are not parallel to those of $-\Delta E_{t,b}^{F\text{-}B}$; hence, tetramers with either the front-to-back or the up-and-down motif alone are not good models for the lipid bilayer. In conclusion, the averaged tetramer model, which combines the front-to-back packing motif with the up-and-down motif, reflects reasonably the multiple lipid-lipid interactions on a relative basis in the gel-state bilayer.

The energy-minimized structures of tetrameric POPCs with Type Ia kink packed in a rectangular box surrounded by 26 exact replicas of image boxes are shown in Fig. 10 *C*. For all four of the lipid species in the large system, the δ_1-, δ_1'-, Δ-, δ_2-, and δ_2'-angles have very similar values; moreover, they are also very similar to the corresponding angles calculated for the monomer before simulations by using periodic boundary conditions. The largest deviation in torsion angle between the energy-minimized monomer and the lipid species in the large system is 11.3°, observed for δ_1-angle in one of the four lipid structures as shown in Table 2. Basically, the structures of various monomeric rotamers obtained by MM calculations are virtually retained in the gel-state bilayer model system.

CONCLUSIONS

In this communication, research has been confined to the identification and characterization of the secondary structural elements or motifs for long hydrocarbon chains each containing a *cis* carbon-carbon double bond. Specifically, four groups of the secondary structural elements are derived for the *sn*-2 acyl chain of a mixed-chain lipid, POPC, at $T < T_m$ using the computer graphics-assisted molecular mechanics method. Within each group, four different types of kink models can arise divergently from a common precursor sequence of the acyl chain.

A common structural feature shared by all *sn*-2 acyl chains of POPC molecules containing different types of Δ-containing kink structure is that the long acyl chain is transformed into two shorter segments. The axes of the two segments and the chain axis of the *sn*-1 acyl chain are typically co-linear. These two shorter segments of the *sn*-2

acyl chain are connected by a linker called the six-atom structural unit. The six-atom structural unit is planar; it consists of two olefinic carbon atoms and two pairs of carbon and hydrogen atoms. Rotations around the carbon-carbon linkages in this six-atom structural unit are paradoxical: the *cis* carbon-carbon double bond (Δ) is essentially immobile, whereas the two carbon-carbon single bonds adjacent to the Δ-bond are highly flexible. In fact, it is the dynamic variations in these bond angles (δ_1 and δ_1') coupled with the neighboring *gauche* bond (δ_2 or δ_2') that facilitate the formation of various types of kink structure in the lipid bilayer.

When POPCs are aggregated to form a closely-packed multiple tetrameric assembly, this assembly is regarded here as a simple model for the gel-state lipid bilayer. The averaged stabilization energies of the lipid bilayers contributed by constituent monomeric species containing various kink structures are compared. Results indicate that these calculated energies are not significantly different, suggesting that the four groups of the secondary structural motif derived in this study can all be present in appreciable amounts in the lipid bilayer at $T < T_m$.

Finally, an inescapable conclusion is the formal recognition of the importance of the *cis* carbon-carbon double bond (Δ) present in mixed-chain phospholipid molecules. From the Δ-bond and other combinations of variables, the secondary structural motifs of lipid acyl chains can be generated readily. Because of the Δ-bond, the *sn*-2 acyl chain of the mixed chain lipid possesses the unique property of being able to assume any one of the mutiple interconverting types of the crankshaft-like kink.

This research was supported, in part, by U. S. Public Health Service Grant GM-17452 from the National Institute of General Medical Sciences, National Institutes of Health, Department of Health and Human Services. The secretarial assistance of Ms. Linda Saunders is gratefully acknowledged.

REFERENCES

Abrahamson, S., and I. Ryderstedt-Nahringbaur. 1962. The crystal structure of the low-melting form of oleic acid. *Acta. Crystallogr.* 15: 1261–1268.

Allinger, N. L. 1977. Conformational analysis. 130. MM2. A hydrocarbon force field utilizing V_1 and V_2 torsional terms. *J. Am. Chem. Soc.* 99: 8127–8134.

Gao, Q., and B. M. Craven. 1986. Conformation of the oleate chains in crystals of cholesteryl oleate at 123K. *J. Lipid Res.* 27:1214–1221.

Huang, C. 1977. A structural model for the cholesterol-phosphatidylcholine complexes in bilayer membranes. *Lipids.* 12:348–356.

Huang, C. 1991. Structures and properties of self-assembled phospholipids in excess water. *In* Phospholipid-Binding Antibodies. E. N. Harris, T. Exner, G. R. V. Hughes, and R. A. Asherson, editors. CRC Press, Boca Raton, FL. 3–30.

Lagaly, G. 1976. Kink-block and gauche-block structures of bimolecular films. *Angew. Chem. Int. Ed. Engl.* 15:575–586.

Lagaly, G., A. Weiss, and E. Stuke. 1977. Effect of double-bonds on bimolecular films in membrane models. *Biochim. Biophys. Acta.* 470: 331–341.

Li, S., Z-q. Wang, H-n. Lin, and C. Huang. 1993. Energy-minimized structures and packing states of a homologous series of mixed-chain phosphatidylcholines: a molecular mechanics study on the diglyceride moieties. *Biophys. J.* 65:1415–1428.

Nakata, Y., A. Takahashi, and T. Takizawa. 1992. Conformational analysis of hexagonal arrangements of phosphatidylcholine headgroups with bound water by molecular mechanics. *J. Chem. Software.* 1:39–44.

Pechhold, W., and S. Blasenbrey. 1967. Kooperative rotationsisomerie in polymeren. I. Schweltztheorie und kinkenkonzehtrationen. *Kolloid Z. Z. Polym.* 216:17:235–244.

Pechhold, W., and S. Blasenbrey. 1970. Molekülbewegung in polymeren. III Teil: mikrostructure und mechanische eigenschaften. *Kolloid Z. Z. Polym.* 241:955–976.

Traüble, H. 1971. The movement of molecules across lipid membrane: a molecular theory. *J. Membr. Biol.* 4:193–208.

Vanderkooi, G. 1991. Multibilayer structure of dimyristoylphosphatidylcholine dihydrate as determined by energy minimization. *Biochemistry.* 30:10760–10768.

Yeagle, P. 1993. The membranes of cells. 2nd Ed. Academic Press, San Diego, CA. 110–112.